

Spectroscopy of nickel monosulfide in 450 – 560 nm by laser-induced fluorescence and dispersed fluorescence techniques

Li Wang, Junfeng Zhen, Jianqiang Gao, Qun Zhang,^{a)} and Yang Chen^{a)}

*Hefei National Laboratory for Physical Sciences at the Microscale and Department of Chemical Physics,
University of Science and Technology of China, Hefei, Anhui 230026, People's Republic of China*

^{a)}Authors to whom correspondence should be addressed. Electronic addresses:
qunzh@ustc.edu.cn and yangchen@ustc.edu.cn

ABSTRACT

Laser-induced fluorescence excitation spectrum of NiS in the wavelength range of 450 – 560 nm has been recorded and analyzed. Fifty-eight vibronic transition bands have been observed, fifty-two of which are reported for the first time. Band-by-band rotational analyses indicated that all the observed bands can be attributable to the ${}^3\Sigma^- - X^3\Sigma^-$ transitions of ${}^{58}\text{NiS}$ (and ${}^{60}\text{NiS}$). Twenty-five bands have been suggested to be grouped into four vibrational progressions. Furthermore, through dispersed fluorescence measurements we directly obtained, for the first time, the energies for the ground-state vibrational levels up to $v''=6$ as well as the vibrational frequency ($\omega_e'' = 506 \pm 5 \text{ cm}^{-1}$) and the anharmonicity constant ($\omega_e''\chi_e'' = 2.29 \pm 0.65 \text{ cm}^{-1}$) for the $X^3\Sigma^-$ ground state of ${}^{58}\text{NiS}$.

I. INTRODUCTION

Transition metal oxides and sulfides have attracted much attention due to their fundamental importance in many fields, such as catalysis,¹ materials science,² high-temperature chemistry,³ and astrophysics.⁴ Transition-metal oxides are commonly used as versatile catalyst in industry, however, non-specific product formation occurs in some processes due to their high reactivity. In contrast, transition-metal sulfides as catalyst are less reactive, hence susceptible to being poisoned and can show higher selectivity. Moreover, transition-metal sulfides are believed to play a crucial role in biochemistry, for they are found in the reaction centers of many enzymes and have even been considered to be essential for the evolution of life.⁵

Over the past years, most of the 3d transition-metal monoxides, such as VO, CrO, MnO, FeO, CoO, NiO, and CuO have been well studied both theoretically and experimentally.⁶⁻¹² However, the spectroscopic data for their monosulfide counterparts are still rather incomplete. Such an incompleteness is even apparent for nickel monosulfide (NiS), in that only the ground state ($X^3\Sigma^-$)¹³ and four excited states (two $^3\Sigma^-$ states and two $^3\Pi$ states)^{14,15} of this species have hitherto been experimentally characterized. By means of source-modulation microwave spectroscopy, Takuya *et al.*¹³ recently observed the rotational spectrum of NiS in the region between 135 and 314 GHz. Their spectral analyses yielded the molecular constants with high precision, such as the rotational, centrifugal distortion, and several fine-structure constants, for the $X^3\Sigma^-$ ground state of NiS. Our group, prior to this microwave work,¹³ has ever reported on a spectroscopic study of NiS by means of laser-induced fluorescence (LIF) technique,¹⁴ in which we tentatively assigned six vibronic

bands newly observed in the wavelength range of 495 and 555 nm as the $[17.4]^3\Sigma^-(\nu'=2-7)-X^3\Sigma^-(\nu''=0)$ transitions. Nevertheless, we recently realized that such an assignment may be questionable, because (1) the ω_e'' value (322 cm^{-1}) used in that assignment¹⁴ was taken from a theoretical prediction¹⁶ which obviously deviates too much from that given in Ref. 13 ($507.227(35)\text{ cm}^{-1}$), a rather convincing value derived from the microwave spectroscopic measurements; (2) the incorrect usage of the ω_e'' value can therefore result in a misleading ν' numbering of the upper $^3\Sigma^-$ electronic state. Furthermore, we detected that the spectroscopic constants for the upper state given in Ref. 14 are also misleading, since the B_0'' value (0.182 cm^{-1})¹⁴ used throughout the whole rotational analyses is too small compared to that given in Ref. 13 (6351.4222 MHz , *i.e.*, 0.21186 cm^{-1}).

We therefore revisited the LIF excitation spectrum of NiS between 495 and 555 nm as reported in Ref. 14, and further extended the laser excitation wavelengths to a broader range, *i.e.*, 450 – 560 nm in this work. Apart from the six vibrational bands reported in Ref. 14, additional 52 bands of NiS were observed for the first time. Based on a global rotational, isotopic shift, and band interval analysis, we assigned 25 out of the 58 bands in total to four progressions with each corresponding to a $^3\Sigma^-(\nu')-X^3\Sigma^-(\nu''=0)$ transition, namely, four upper electronic states of NiS with an identical symmetry of $^3\Sigma^-$ were identified in the energy range of ~ 18100 and 22100 cm^{-1} (*i.e.*, 450 – 560 nm). As the B_0'' value given in Ref. 13 was used throughout the rotational analyses in the present work, reliable rotational constants were obtained for the upper vibronic states related to all the 58 bands, among which those for the six bands reported in Ref. 14 were corrected. Furthermore, we recorded the dispersed fluorescence (DF) spectra at two differing excitation wavelengths, from which

the energies for the ground-state vibrational levels up to $v''=6$ were determined. The DF measurements also allowed us to obtain experimentally, for the first time, the vibrational frequency ($\omega_e'' = 506 \pm 5 \text{ cm}^{-1}$) and the anharmonicity constant ($\omega_e \chi_e'' = 2.29 \pm 0.65 \text{ cm}^{-1}$) for the $X^3\Sigma^-$ ground state of ^{58}NiS .

II. EXPERIMENT

The experimental apparatus has been described in detail elsewhere.¹⁷⁻¹⁹ Briefly, the NiS molecules were produced by the reaction of H_2S molecules with the nickel atoms sputtered from a pair of pure nickel pin electrodes under a pulsed DC discharge condition. The H_2S sample seeded in argon ($\sim 2\%$) at a stagnation pressure of ~ 5 atm passed through a pulsed nozzle (General Valve Co.) with an orifice diameter of 0.5 mm into the vacuum chamber. The nickel pins used for DC discharging the $\text{H}_2\text{S}/\text{Ar}$ gas was fixed in a Teflon disk, and set at a spacing of ~ 1 mm. The background pressure of the vacuum chamber was $\sim 4 \times 10^{-4}$ and $\sim 3 \times 10^{-5}$ Torr, with and without operation of the free jet, respectively.

The light source used was a tunable dye laser (Lumonics, HT-500) pumped by a Nd:YAG laser (Spectra Physics, GCR-190). The output of the pulsed dye laser (linewidth $\sim 0.1 \text{ cm}^{-1}$, pulse duration ~ 5 ns) was introduced into the vacuum chamber and crossed the jet flow perpendicularly about 3 cm downstream from the point of discharge.

The LIF excitation spectra were recorded by monitoring the total fluorescence as a function of laser wavelength. No attempt was made to normalize the spectral intensity against the laser power. The DF spectra were obtained by fixing the probe laser frequency at or near a strong R -head and scanning the monochromator (Zolix, Omni- λ 300) with a

1-mm-wide slit. The relative time delays among the nozzle, the laser, and the discharge were controlled by a multichannel pulsed delay generator. Laser wavelengths were calibrated by a wavemeter (Coherent, WaveMaster 33-2650).

III. RESULTS AND DISCUSSION

Figure 1 shows a survey LIF excitation spectrum of NiS in the laser wavelength range of 450 – 560 nm. This spectrum is very complex (comprising 58 rotationally analyzable bands), which may result from the presence of huge numbers of the low-lying electronic states and the widespread perturbations among the electronic states; spin multiplicity may add more complexity to the spectrum.¹⁴ Apart from the spectral features arising from ⁵⁸NiS, those arising from its isotopic molecule ⁶⁰NiS were also observed (natural abundance ratio of ⁵⁸Ni/⁶⁰Ni ~ 2.6:1).

Through band-by-band rotational analyses (examples see below), we found that all the observed 58 bands shown in Fig. 1 can be attributed to the $^3\Sigma^- - ^3\Sigma^-$ type transition. Since all the NiS molecules in the detection zone are in their ground state after having expanded for $\sim 60 \mu\text{s}$ from the discharge zone in our experiment, we can conclude that all the vibronic bands observed in this work should originate from the ground state of NiS.¹³

A focus on band-head positions suggests four groupings of bands: (i) a progression from 550.96 nm, namely bands at 550.96, 540.24, 531.01, 521.53, 512.19, 503.67, 494.65, and 485.80 nm. These bands occur at intervals of $\sim 348 \text{ cm}^{-1}$. The bands labeled (i)'s in the lower panel of Fig. 1 are those observed previously (with similar intervals of $\sim 340 \text{ cm}^{-1}$ ¹⁴); (ii) a progression from 508.89 nm, namely bands at 508.89, 499.53, 490.73, 481.90, 473.75, and

465.81 nm. These bands occur at intervals of $\sim 363 \text{ cm}^{-1}$; (iii) a progression from 493.17 nm, namely bands at 493.17, 484.61, 476.62, 468.73, 461.18, and 453.73 nm. These bands occur at intervals of $\sim 352 \text{ cm}^{-1}$; (iv) a progression from 496.21 nm, namely bands at 496.21, 487.54, 479.31, 471.58, and 463.60 nm. These bands occur at intervals of $\sim 354 \text{ cm}^{-1}$.

The 25 vibronic bands grouped into the four progressions are labeled correspondingly (i), (ii), (iii), and (iv) in Fig. 1. Since perturbations among excited states are widespread,^{14,15} which leads to irregularities in the isotope shifts as well as the rotational constants obtained from our rotational analyses for these bands, we here adopt the above tentative classification, as did in a recent report on NiO by Balfour *et al.*¹¹ We thus hold that the ν' numbering given in Ref. 14 (*i.e.*, the assignments of $[17.4]^3\Sigma^-(\nu'=2-7)-X^3\Sigma^-(\nu''=0)$ for the six bands labeled (i)'s in the lower panel of Fig. 1) is doubtful, as has been stated in the Introduction section.

Listed in Table I are the observed band heads (λ_{head}) together with the band origins (ν_0) obtained from the rotational analyses for the 25 bands belonging to the four vibrational progressions. As the four progressions have been identified (through rotational analyses given below) as being due to the $^3\Sigma^- - ^3\Sigma^-$ transition, the vibrational frequencies (ω_e') of the four newly observed $^3\Sigma^-$ excited states can be estimated to be $\sim 350 \text{ cm}^{-1}$; however, the accurate ω_e' (and $\omega_e\chi_e'$) values for the four $^3\Sigma^-$ states cannot be determined in the present work, partly because of the unidentified ν' numbering.

It is noteworthy that there remain 33 bands unlabeled in Fig. 1. Through careful rotational analyses we confirmed that the 33 rotationally analyzable bands, similar to the aforementioned 25 bands (labeled (i) – (iv) in Fig. 1), should also originate from the

${}^3\Sigma^- - {}^3\Sigma^-$ type transition. Nevertheless, they can neither be classified into the four groupings shown in Fig. 1 nor into any other vibrational progressions; this sort of perturbation-induced spectral complexity can also be found in other 3d transition-metal diatomic molecules (*e.g.*, NiO¹¹). Table II lists the band heads (λ_{head}) together with the band origins (ν_0) for the 33 bands not belonging to the four vibrational progressions.

The band-by-band rotational analyses indicated that all the 58 vibrational bands of NiS show a similar R - P rotational structure, as can be seen in the 503.67 nm ($\sim 19854.27 \text{ cm}^{-1}$) band (*i.e.*, the band labeled (a) in Fig. 1) and the 459.54 nm ($\sim 21760.89 \text{ cm}^{-1}$) band (*i.e.*, the band labeled (b) in Fig. 1) shown in Figs. 2 and 3, respectively. The two bands are representative of those in and out of the four vibrational progressions described above, respectively. From Figs. 2 and 3 we can readily detect that both spectra exhibit P and R (without Q) branches and that P branch merges with a sharp R head, which indicates to a $\Sigma - \Sigma$ type transition. Since the ground state of NiS has been determined to be of ${}^3\Sigma^-$ symmetry,¹³ we can reasonably attribute all the observed 58 bands shown in Fig. 1 to the ${}^3\Sigma^- - X{}^3\Sigma^-$ transitions. Very weak though compared to those from ${}^{58}\text{NiS}$, the spectral features arising from ${}^{60}\text{NiS}$ are discernible, as shown in Figs. 2 and 3, which in turn confirms that the spectral carrier is indeed NiS.

The upper part of Figs. 2 and 3 shows the observed spectrum of both ${}^{58}\text{NiS}$ and ${}^{60}\text{NiS}$ with P and R branches indicated by ticks showing corresponding J numbers. Table III lists rotational assignments for the 503.67 nm and 459.54 nm bands, the bands labeled (a) and (b) in Fig. 1, respectively. Note that the rotational lines with $J > 25$ in Figs. 2 and 3 can rarely be measured because of the jet-cooled conditions in our experiment. A least-squares fit

with the PGOPHER program²⁰ allowed us to simulate the rotational spectra. The simulated spectra (shown in the lower part of Figs. 2 and 3) match nicely with the observed ones, which further supports our spectral assignments.

The data derived from the rotational analyses, including the band origins (ν_0), the rotational constants (B'), $\Delta B = B' - B''$, and the isotope shifts ($\Delta\nu_0^i = \nu_0(^{58}\text{NiS}) - \nu_0(^{60}\text{NiS})$), are listed in Tables I and II. Note that (1) for each of the four vibrational progressions, the $\Delta\nu_0^i$ values given in Table I do not exhibit good linear relationship with band positions; and (2) there remain some vacancies for the $\Delta\nu_0^i$ values in Table II. These may be interpreted in terms of widespread perturbations among excited states^{11,14,15} and perturbation-induced spectral congestion.

In addition to the above LIF work pertinent to the newly identified $^3\Sigma^-$ excited states of NiS in the wavelength range of 450 – 560 nm, we further recorded the dispersed fluorescence (DF) spectra at two differing excitation wavelengths in an attempt to directly acquire information about the $X^3\Sigma^-$ ground state of NiS. In two of the progressions identified above, the lead bands, specifically those at 503.67 nm (labeled (a) in Fig. 1) and 476.62 nm (labeled (c) in Fig. 1), are among the strongest members. DF spectra were recorded with probe laser excitation fixed to coincide with the most intense *R*-head in the ^{58}NiS isotopomer of each band.

Figure 4, as an example, shows thus obtained DF spectrum with excitation wavelength (λ_{exc}) fixed at 476.62 nm. The displacements of the seven peaks in Fig. 4, with respect to the position marked with an arrow, read 0, 505, 1002, 1495, 1988, 2479, and 2952 cm^{-1} , respectively. [Note: The DF spectrum recorded with $\lambda_{exc} = 503.67$ nm was qualitatively

similar.] The predominant emission was found at ~ 476.62 nm, exactly equivalent to the wavelength used for excitation, which implies that this strongest peak should correspond to the ${}^3\Sigma^-(\nu') \rightarrow X^3\Sigma^-(\nu''=0)$ transition. We thereby anticipate that the remaining six peaks may correspond to the ${}^3\Sigma^-(\nu') \rightarrow X^3\Sigma^-(\nu''=1-6)$ transitions. Fitting the above displacement values into the customary equation $G(\nu'') = \omega_e''(\nu'' + \frac{1}{2}) - \omega_e x_e''(\nu'' + \frac{1}{2})^2$ yields the vibrational frequency ($\omega_e'' = 506 \pm 5$ cm $^{-1}$) as well as the anharmonicity constant ($\omega_e x_e'' = 2.29 \pm 0.65$ cm $^{-1}$) for the $X^3\Sigma^-$ ground state of ${}^{58}\text{NiS}$. These two vibrational constants we obtained directly from our DF measurements turned out to agree reasonably with the calculated ones ($\omega_e'' = 507.227 \pm 0.035$ cm $^{-1}$ and $\omega_e x_e'' = 2.20341 \pm 0.00038$ cm $^{-1}$) that were based on the microwave spectroscopic data (B_e'' , D_e'' , and α_e'')¹³ and usage of the equations $\omega_e'' = \sqrt{\frac{4B_e''^3}{D_e''}}$ and $\omega_e x_e'' = B_e''(\frac{\alpha_e'' \omega_e''}{6B_e''^2} + 1)^2$. Such an agreement further supports our LIF work described above. To the best of our knowledge, the DF work presented here represents a first direct measurement of the vibrational energies and the two vibrational constants (ω_e'' and $\omega_e x_e''$) for the $X^3\Sigma^-$ ground state of ${}^{58}\text{NiS}$.

IV. CONCLUSIONS

The jet-cooled laser-induced fluorescence excitation spectrum of NiS has been investigated between 450 and 560 nm where fifty-eight vibronic transition bands have been observed. All these bands have been assigned as the ${}^3\Sigma^- - X^3\Sigma^-$ transitions based on our band-by-band rotational and isotopic shift analyses. Four vibrational progressions involving twenty-five bands are suggested. Dispersed fluorescence spectra we recorded at two differing excitation wavelengths map the ground-state vibrational levels up to $\nu'' = 6$,

from which the experimentally derived values of the ^{58}NiS ground-state vibrational frequency ($\omega_e'' = 506 \pm 5 \text{ cm}^{-1}$) and anharmonicity constant ($\omega_e \chi_e'' = 2.29 \pm 0.65 \text{ cm}^{-1}$) have been given for the first time.

ACKNOWLEDGEMENTS

We gratefully acknowledge partial support from the National Natural Science Foundation of China (Grant Nos. 20673107 and 20873133), the Ministry of Science and Technology of China (Grant Nos. 2007CB815203 and 2010CB923300), the Chinese Academy of Sciences (KJCX2-YW-N24), and the Scientific Research Foundation for the Returned Overseas Chinese Scholars, Ministry of Education of China.

References

- ¹G. D. Cody, *Annu. Rev. Earth Planet. Sci.* **32**, 569 (2004).
- ²C. W. Bauschlicher Jr. and P. Maitre, *Theor. Chim. Acta* **90**, 189 (1995).
- ³H. Spinrad and R. F. Wing, *Annu. Rev. Astron. Astrophys.* **7**, 249 (1969).
- ⁴A. J. Merer, *Annu. Rev. Phys. Chem.* **40**, 407 (1989).
- ⁵I. Kretzschmar, D. Schröder, H. Schwarz, and P. B. Armentrout, in *Advances in Metal and Semiconductor Clusters – Metal-Ligand Bonding and Metal-Ion Solvation* **5**, 347 (2001).
- ⁶L. Karlsson, B. Lindgren, C. Lundevall, and U. Sassenberg, *J. Mol. Spectrosc.* **181**, 274 (1997).
- ⁷M. Barnes, P. G. Hajigeorgiou, and A. J. Merer, *J. Mol. Spectrosc.* **160**, 289 (1993).
- ⁸K. M. Green, R. P. Kampf, and J. M. Parson, *J. Chem. Phys.* **112**, 1721 (2000).
- ⁹M. Barnes, M. M. Fraser, P. G. Hajigeorgiou, A. J. Merer, and S. D. Rosner, *J. Mol. Spectrosc.* **170**, 449 (1995).
- ¹⁰M. Barnes, D. J. Clouthier, P. G. Hajigeorgiou, G. Huang, C. T. Kingston, A. J. Merer, G. F. Metha, J. R. D. Peers, and S. J. Rixon, *J. Mol. Spectrosc.* **186**, 374 (1997).
- ¹¹W. J. Balfour, J. Cao, R. H. Jensen, and R. Li, *Chem. Phys. Lett.* **385**, 239 (2004).
- ¹²O. Appelblad, A. Lagerqvist, I. Renhorn, and R. W. Field, *Phys. Scr.* **22**, 603 (1981).
- ¹³T. Yamamoto, N. Tanimoto, T. Okabayashi, *Phys. Chem. Chem. Phys.* **9**, 3744 (2007).
- ¹⁴X. F. Zheng, T. T. Wang, J. R. Guo, C. X. Chen, and Y. Chen, *Chem. Phys. Lett.* **394**, 137 (2004).
- ¹⁵J. F. Zhen, L. Wang, C. B. Qin, Q. Zhang, and Y. Chen, *Chin. J. Chem. Phys.* **22**, 668 (2009).

- ¹⁶A. I. Boldyrev and J. Simons, *Periodic Table of Diatomic Molecules* (Wiley, New York, 1997).
- ¹⁷Y. Chen, J. Jin, C. J. Hu, X. L. Yang, X. X. Ma, and C. X. Chen, *J. Mol. Spectrosc.* **203**, 37 (2000).
- ¹⁸J. Jin, Q. Ran, X. L. Yang, Y. Chen, and C.X. Chen, *J. Phys. Chem. A* **105**, 11177 (2001).
- ¹⁹X. P. Zhang, J. R. Guo, T. T. Wang, L. S. Pei, Y. Chen, and C. X. Chen, *J. Mol. Spectrosc.* **220**, 209 (2003).
- ²⁰C. M. Western, *PGOPHER: A Program for Simulating Rotational Structure* (Univ. of Bristol, <http://pgopher.chm.bris.ac.uk>).

Figure Captions

FIG. 1. (Color online) The survey LIF excitation spectrum of NiS in the wavelength range of 450 – 560 nm. The 25 bands labeled (i), (ii), (iii), and (iv) are those can be grouped into four progressions, while the remaining 33 bands are not labeled. [See text for details.] The two bands indicated by (a) and (b) are presented in more detail in Figs. 2 and 3, respectively. (c) indicates the band whose band head is chosen to be the excitation wavelength (476.62 nm) for the DF measurement shown in Fig. 4.

FIG. 2. (Color online) Rotationally resolved LIF excitation spectrum of NiS near 503.67 nm (*i.e.*, the band labeled (a) in Fig. 1). The upper trace is the observed spectrum; while the lower trace is the simulated spectrum.

FIG. 3. (Color online) Rotationally resolved LIF excitation spectrum of NiS near 459.54 nm (*i.e.*, the band labeled (b) in Fig. 1). The upper trace is the observed spectrum; while the lower trace is the simulated spectrum.

FIG. 4. The DF spectrum of ^{58}NiS obtained using a probe laser wavelength fixed at 476.62 nm, which corresponds to the band-head position of the band labeled (c) in Fig. 1. This spectrum can be readily interpreted in terms of emission solely into the vibrational manifold ($\nu''=0-6$ as indicated by ticks) of the electronic ground state.

Table Legends

TABLE I. ^{58}NiS band heads (λ_{head} , in nm), band origins (ν_0 , in cm^{-1}), rotational constants (B' , in cm^{-1}), $\Delta B = B' - B''^{(a)}$ (cm^{-1}), and $^{58}\text{NiS}/^{60}\text{NiS}$ isotopic shifts ($\Delta\nu_0^i$, in cm^{-1}) for the 25 bands belonging to the four vibrational progressions (see text). Several $\Delta\nu_0^i$ values with question mark remain doubtful (see discussion in the text).

^(a) B'' was fixed at 0.21186 cm^{-1} (adopted from [Ref. 13](#)).

TABLE II. ^{58}NiS band heads (λ_{head} , in nm), band origins (ν_0 , in cm^{-1}), rotational constants (B' , in cm^{-1}), $\Delta B = B' - B''^{(a)}$ (cm^{-1}), and $^{58}\text{NiS}/^{60}\text{NiS}$ isotopic shifts ($\Delta\nu_0^i$, in cm^{-1}) for the 33 bands not belonging to the four vibrational progressions (see text).

^(a) B'' was fixed at 0.21186 cm^{-1} (adopted from [Ref. 13](#)).

TABLE III. Rotational assignments (cm^{-1}) in the 503.67 and 459.54 nm bands of ^{58}NiS and ^{60}NiS .

Fig. 1 (Wang *et al.*)

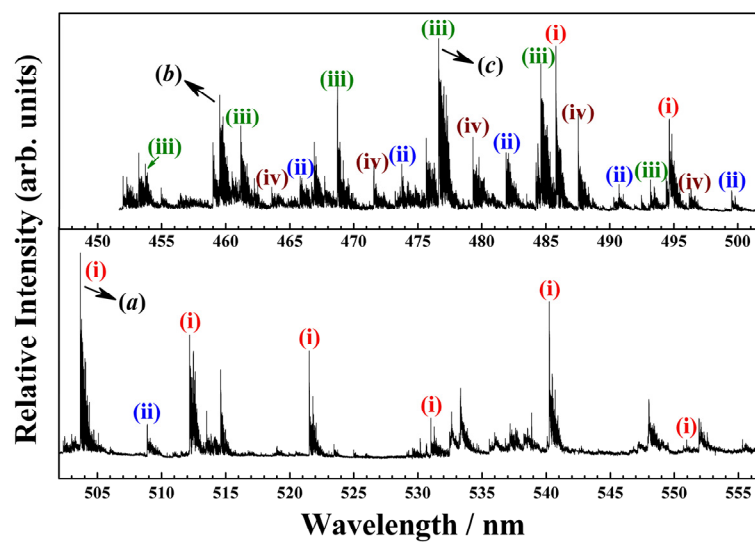


Fig. 2 (Wang *et al.*)

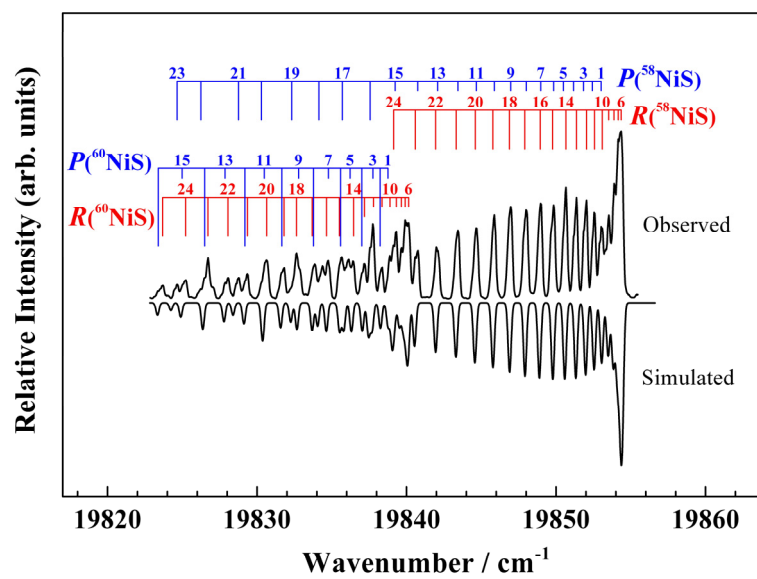


Fig. 3 (Wang *et al.*)

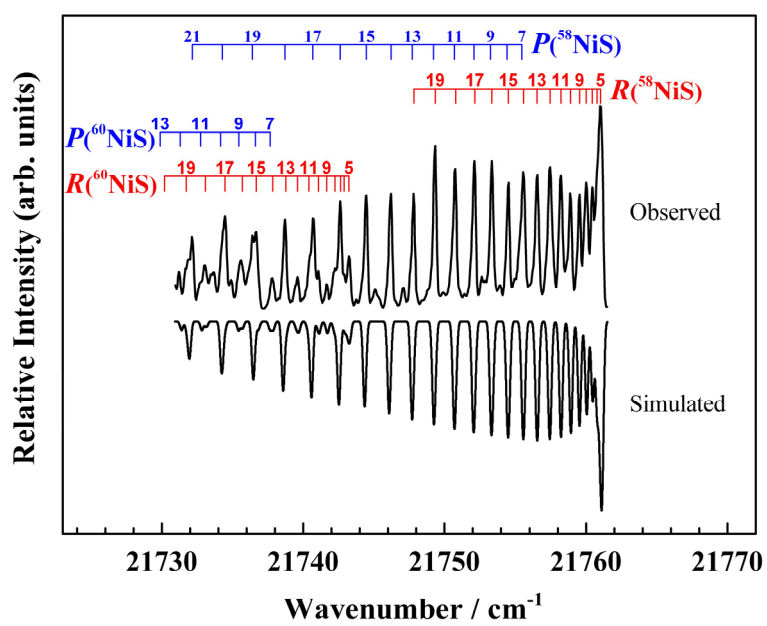


Fig. 4 (Wang *et al.*)

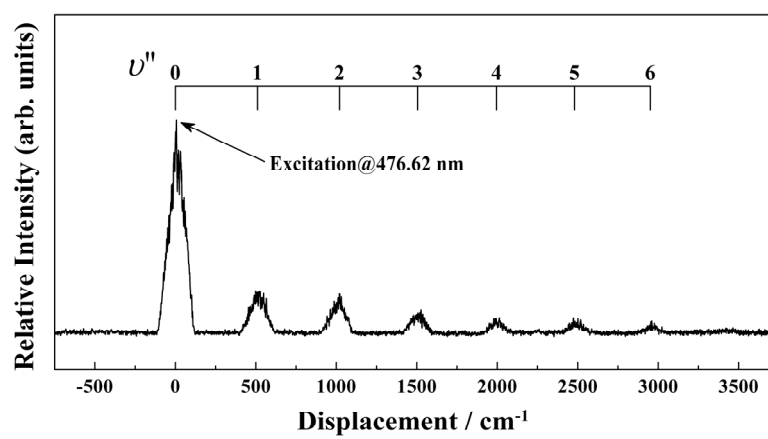


TABLE I

λ_{head} (nm)	ν_0 (cm^{-1})	B' (cm^{-1})	$B' - B''$ (cm^{-1})	$\Delta\nu_0^i$ (cm^{-1})
550.96	18149.4	0.1730	-0.0389	4.54
540.24	18509.3	0.1734	-0.0385	8.10
531.01	18831.2	0.1725	-0.0394	9.56
521.53	19173.5	0.1714	-0.0405	10.46
512.19	19523.2	0.1735	-0.0384	20.53?
508.89	19649.6	0.1710	-0.0409	8.35
503.67	19853.5	0.1732	-0.0387	14.31
499.53	20018.0	0.1676	-0.0443	10.56
496.21	20151.9	0.1695	-0.0424	16.08
494.65	20215.3	0.1707	-0.0412	7.70?
493.17	20276.1	0.1682	-0.0437	12.39
490.73	20377.3	0.1669	-0.0450	14.31
487.54	20510.3	0.1710	-0.0409	17.86
485.80	20584.0	0.1688	-0.0431	16.71
484.61	20634.1	0.1698	-0.0421	20.26?
481.90	20750.4	0.1649	-0.0470	13.48
479.31	20862.4	0.1663	-0.0456	20.15
476.62	20980.1	0.1712	-0.0407	16.60
473.75	21107.4	0.1697	-0.0422	19.20
471.58	21204.6	0.1682	-0.0437	16.18
468.73	21333.3	0.1697	-0.0422	17.07
465.81	21467.3	0.1623	-0.0496	11.27
463.60	21569.5	0.1684	-0.0435	10.47
461.18	21682.7	0.1695	-0.0424	23.07
453.73	22038.7	0.1710	-0.0409	12.81?

TABLE II

λ_{head} (nm)	ν_0 (cm^{-1})	B' (cm^{-1})	$B' - B''$ (cm^{-1})	$\Delta\nu_0^i$ (cm^{-1})
555.33	18006.4	0.1799	-0.0320	5.28
551.93	18117.3	0.1798	-0.0321	4.84
548.02	18246.8	0.1773	-0.0346	
538.55	18567.9	0.1705	-0.0414	
537.18	18614.9	0.1763	-0.0356	15.27
535.57	18670.8	0.1730	-0.0389	7.63
533.32	18749.4	0.1793	-0.0326	10.35
532.62	18774.0	0.1780	-0.0339	
529.59	18881.7	0.1761	-0.0358	11.37
524.99	19046.9	0.1763	-0.0356	
523.45	19103.3	0.1693	-0.0426	10.72
519.01	19266.4	0.1794	-0.0325	
514.62	19430.9	0.1737	-0.0382	13.35
513.51	19472.7	0.1799	-0.0320	13.69
502.45	19901.5	0.1700	-0.0419	7.30
492.48	20304.8	0.1699	-0.0420	
491.93	20327.3	0.1771	-0.0348	5.49
475.66	21022.7	0.1661	-0.0458	22.03
475.33	21037.5	0.1702	-0.0417	
474.80	21060.9	0.1693	-0.0426	
474.22	21086.5	0.1732	-0.0387	
473.25	21129.8	0.1707	-0.0412	8.60
467.72	21379.5	0.1748	-0.0371	21.69
466.92	21416.1	0.1661	-0.0458	16.06
466.29	21445.2	0.1688	-0.0431	10.45
460.51	21714.1	0.1692	-0.0427	
459.54	21760.4	0.1657	-0.0462	17.86
459.01	21785.4	0.1671	-0.0448	9.38
456.47	21906.7	0.1683	-0.0436	19.09
454.96	21979.1	0.1668	-0.0451	15.15
453.20	22064.4	0.1667	-0.0452	
452.26	22110.3	0.1637	-0.0482	23.53
451.99	22123.8	0.1680	-0.0439	

TABLE III

<i>J</i>	⁵⁸ NiS		⁶⁰ NiS	
	<i>R(J)</i>	<i>P(J)</i>	<i>R(J)</i>	<i>P(J)</i>
(a) 503.67 nm band				
1		19853.02		19838.76
2		19852.43		19838.23
3		19851.84		19837.75
4		19851.17		19837.01
5		19850.49		19836.22
6	19854.36	19849.84	19840.14	19835.59
7	19854.16	19848.98	19839.91	19834.77
8	19853.88	19848.01	19839.65	19833.78
9	19853.52	19846.97	19839.32	19832.78
10	19853.09	19845.87	19838.89	19831.66
11	19852.57	19844.67	19838.36	19830.48
12	19852.04	19843.44	19837.79	19829.19
13	19851.37	19842.08	19837.18	19827.86
14	19850.66	19840.75	19836.46	19826.50
15	19849.77	19839.24	19835.51	19824.99
16	19848.94	19837.56	19834.65	19823.39
17	19847.91	19835.71	19833.69	
18	19846.88	19834.14	19832.64	
19	19845.77	19832.32	19831.80	
20	19844.60	19830.29	19830.65	
21	19843.32	19828.76	19829.36	
22	19841.94	19826.25	19828.06	
23	19840.59	19824.65	19826.72	
24	19839.14		19825.22	
25			19823.68	
(b) 459.54 nm band				
1				
2				
3				
4				
5	21761.03		21743.24	
6	21760.77		21742.88	
7	21760.44	21755.47	21742.63	21737.67
8	21760.01	21754.43	21742.25	21736.63
9	21759.54	21753.25	21741.67	21735.44
10	21758.89	21752.07	21741.06	21734.16
11	21758.22	21750.70	21740.40	21732.74

12	21757.45	21749.24	21739.60	21731.30
13	21756.55	21747.72	21738.77	21729.89
14	21755.59	21746.21	21737.85	
15	21754.51	21744.44	21736.67	
16	21753.36	21742.62	21735.68	
17	21752.13	21740.69	21734.47	
18	21750.78	21738.71	21733.09	
19	21749.35	21736.41	21731.74	
20	21747.84	21734.27	21730.19	
21		21732.15		
22		21729.79		
